

Short communication

## The Electrocatalytic Activity of the Pyrolysis Products of the Mixture Containing PdO and PdCl<sub>2</sub> and Multi-walled Carbon Nanotubes (MWCNTs) for Methanol Oxidation Reaction (MOR)

Keqiang Ding<sup>1,3,\*</sup>, Yan Zhang<sup>1</sup>, Sen Li<sup>3</sup>, Binjuan Wei<sup>1</sup>, Pingyuan Wang<sup>2</sup>, Junqing Pan<sup>2,\*</sup>

<sup>1</sup>College of Chemistry and Materials Science, Hebei Normal University, Shijiazhuang 050024, P.R. China

<sup>2</sup>State Key Laboratory of Chemical Resource Engineering, Beijing University of Chemical Technology, Beijing, 100029, China

<sup>3</sup>Fengfan Co., Ltd, Baoding, Hebei 071057, P.R. China

\*E-mail: [dkeqiang@263.net](mailto:dkeqiang@263.net), [jqpan@mail.buct.edu.cn](mailto:jqpan@mail.buct.edu.cn)

Received: 15 December 2016 / Accepted: 4 January 2017 / Published: 12 February 2017

---

In this work, three kinds of catalysts were respectively prepared from the mixture of PdO+PdCl<sub>2</sub>+MWCNTs (catalyst a), PdCl<sub>2</sub>+MWCNTs (catalyst b) and PdO+MWCNTs (catalyst c) by using a pyrolysis method. And their characterizations were basically conducted via X-ray diffraction (XRD) and transmission electron microscopy (TEM). The XRD results indicated that metallic Pd as the main component was prepared in catalyst a and b. The particle size for catalyst a, b and c was approximately estimated to be 15nm, 10nm and 20 nm, respectively, basing on the TEM images. And the electrocatalytic activities of the obtained catalysts for methanol oxidation reaction (MOR) were investigated mainly through cyclic voltammetry (CV) and chronoamperometry (CA). And the results effectively illustrated that catalyst a showed the best electrocatalytic activity toward MOR among all the prepared catalysts. Showing the fact, that the pyrolysis products of the mixture having PdO and PdCl<sub>2</sub> and MWCNTs had an unexpected electrocatalytic activity towards MOR, is the main contribution of this work, which can greatly reduce the preparation cost of Pd-based catalyst.

---

**Keywords:** PdO, PdCl<sub>2</sub>, pyrolysis; multi-walled carbon nanotubes; electrocatalyst; methanol oxidation reaction.

### 1. INTRODUCTION

Recently, the research works concerning the electrocatalysts of methanol oxidation reaction (MOR) have been paid much more attention mainly due to the pivotal role of MOR in the direct

methanol fuel cells (DMFCs) [1]. In the anodic chamber of DMFCs, electrons can be released from the electro-oxidation of methanol, and in the cathodic part, those released electrons may react with oxygen (oxygen gas was from air) to generate the superoxide anion of  $O_2^-$ , leading to the formation of an electronic circuit. Of late, numerous research works concerning the catalysts of MOR have indicated that MOR can only proceed on the Pt or Pd based composites (or alloys), thus, developing a simple way to produce Pt or Pd based catalysts became very attractive for the catalyst-related electrochemistry researchers [2]. Meanwhile, the main drawbacks of using Pt as electrocatalyst for MOR, such as the higher cost and limited reserves of Pt, were claimed by many research groups very recently. Thus, Pd or Pd-based catalysts, mainly due to their lower cost and abundant reserves, as well as the acceptable electrocatalytic activity for MOR compared to the Pt-based catalysts especially in alkaline media, have attracted a great deal of attention peculiarly in the research field of anodic electrocatalyst for MOR [3]. Although many kinds of Pd-based catalyst were generated in recent years, the complicated synthetic process and synthetic cost have greatly hindered the final commercialization of those Pd-based electrocatalyst. That is to say, preparation cost and manufacturing process as well as the properties of catalysts are the three main factors which can directly decide the commercial value of a novel catalyst. Or in other words, developing novel method to prepare Pd-based catalyst with lower cost and satisfactory electrocatalytic activity is still a hot topic in the electrocatalyst research field.

It is well known that the chemical reduction method [4] and the electrochemical method [5] are the two main typical methods for preparing Pd-based catalysts. Evidently, one kind of reducing agent was required in the chemical reduction method [4], and an external power was needed in the electrochemical method [5]. Compared to above two preparation methods, pyrolysis method was a very simple way which is generally called as one-pot reaction. Our former work [6] has indicated that MWCNTs itself could be employed as a reducing agent in the pyrolysis preparation of Pd-based catalyst. However, to the best of our knowledge, the preparation of metallic Pd nanoparticles from the mixture containing PdO and PdCl<sub>2</sub> and MWCNTs using a pyrolysis method has not been reported to date.

In this work, three kinds of mixture, i.e., PdO+PdCl<sub>2</sub>+MWCNTs, PdCl<sub>2</sub>+MWCNTs and PdO+MWCNTs, were made first, and then, after a very simple method of pyrolysis, three kinds of catalysts were generated. Interestingly, all these three catalysts showed electrocatalytic activities for MOR, and catalyst a displayed the best electrocatalytic ability among the obtained three catalysts. This work is believed to be very helpful for the development of electrocatalyst for MOR, due to its very simple manipulation steps and acceptable electrocatalytic activity.

## 2. EXPERIMENTAL

### 2.1 Materials

MWCNTs with a diameter ranging from 10 nm to 20 nm were bought from Shenzhen nanotech port Co., Ltd. (China). All the electrodes were provided by Tianjin Aida Co., Ltd (China). All the

chemicals with analytical grade were used as-received. Doubly distilled water was utilized to produce the aqueous solutions.

### 2.2 Preparation of pyrolysis products

Firstly, 12.0 mg PdO, 17.7 mg PdCl<sub>2</sub> and 10.0 mg MWCNTs (the atomic ratio of Pd in PdO to Pd in PdCl<sub>2</sub> was close to 1:1) were together added into 4 mL doubly distilled water, forming a suspension solution. Afterwards, the resultant suspension solution was treated with ultrasonication for 30 min to generate a more homogeneous phase. Secondly, the prepared suspension solution was placed in a home-made and well-sealed autoclave, and then the autoclave was put in a muffle furnace. Subsequently, the muffle furnace was maintained at 200 °C for 2 h to complete the pyrolysis process. Lastly, after the temperature of the autoclave was close to the room temperature, the produced catalysts were filtered with copious distilled water, and dried in air leading to the formation of catalyst a. Similarly, catalyst b and c were also prepared using above preparation process. Summarily, catalyst a, b and c corresponded to the pyrolysis products from the mixture of PdO+PdCl<sub>2</sub>+MWCNTs, PdCl<sub>2</sub>+MWCNTs and PdO+MWCNTs, respectively.

### 2.3 Preparation of catalyst coated GC electrode

Firstly, 1 mg of above prepared catalyst was dispersed into 1 mL Nafion ethanol solution (The mass content of Nafion was 0.1 wt.%), which was followed by 20 min ultrasonication, leading to the formation of a catalyst ink. Secondly, 15 μL catalyst ink was dropped onto a well-polished glassy carbon (GC) electrode (diameter was 3 mm). And after drying in air, the catalyst coated GC electrode was produced. The GC electrodes coated with catalyst a, b and c were denoted as electrode a, b and c, respectively.

In this experiment, the working electrode, reference electrode and counter electrode was the catalyst coated GC electrode, saturated calomel electrode (SCE) and platinum wire, respectively. The electrolyte solution used was 1 M KOH +1M CH<sub>3</sub>OH.

### 2.4 Characterizations

The composition and the crystallinity of the prepared catalysts was analyzed by using a Bruker D8 ADVANCE X-ray diffractometer (XRD) with a Cu Kα source ( $\lambda = 0.154$  nm) at 40 kV and 30 mA. The morphologies of the prepared catalysts were studied by using transmission electron microscopy (TEM, HITACHI, H-7650). Energy Dispersive X-Ray Spectroscopy (EDS) spectrum analysis was performed on a X-ray energy instrument (EDAX, PV-9900, USA). Electrochemical measurements were conducted on a CHI 660B electrochemical working station (Shanghai Chenhua Apparatus, China) that was controlled by a personal computer.

In the electrochemical measurements, a conventional three-electrode cell was employed. The electrocatalytic activity of the prepared catalysts towards MOR was examined in a solution of 1 M

KOH containing 1 M CH<sub>3</sub>OH. The synthesized catalyst coated GC electrode, a platinum wire and a saturated calomel electrode (SCE) were, employed as the working electrode, counter electrode and reference electrode, respectively. All the potentials reported in this work were in terms of the electrode potential value of the SCE electrode. All the experiments were conducted at room temperature.

### 3. RESULTS AND DISCUSSION

#### 3.1 XRD analysis

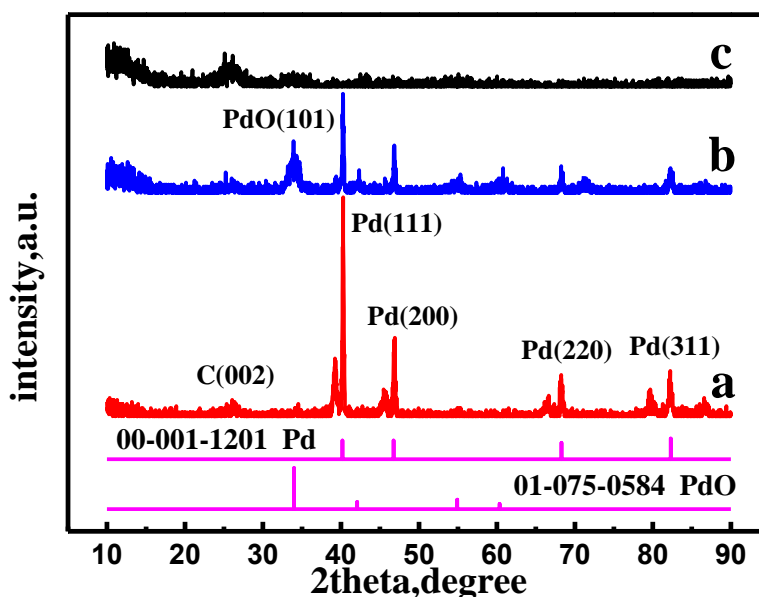


**Figure 1.** XRD patterns of the obtained catalysts. Pattern a, b and c corresponded to catalyst a, b and c.

To investigate the composition and crystallinity of the prepared catalysts, XRD analysis was made first and the results are illustrated in Fig.1. According to the previous work of MWCNTs, the small diffraction peak observed at about 26.0° should be assigned to carbon facet of (002) for the MWCNTs [7], indicating the presence of MWCNTs in final products. Evidently, except for the (002) crystal plane of MWCNTs, no other diffraction peaks were found in the XRD pattern for catalyst c, which indicated that the synthesized substance in catalyst c was amorphous. Careful observation revealed that four typical diffraction peaks of metallic Pd [8] (JCPDS, No. 00-001-1201), namely, 39.1° (111), 45.3° (200), 66.2° (220) and 79.8° (311), were all exhibited in the prepared catalyst a and b. It strongly demonstrated that the metallic Pd as the main component was contained in the prepared catalyst a and b. Meanwhile, the intensity of the diffraction peak for the metallic Pd in catalyst a was much higher than that of catalyst b, which may promise that the electrocatalytic activity of catalyst a was superior to that of catalyst b. XRD patterns shown in Fig.1 effectively proved that it was a feasible way for producing metallic Pd by a very simple method of pyrolysis using PdO and PdCl<sub>2</sub> as the starting materials in the presence of MWCNTs.

3.2 Morphology characterization

TEM images for all the prepared catalysts are given in Fig. 2. Apparently, in all images, MWCNTs are exhibited clearly demonstrating that the main morphology of MWCNTs was not damaged in the pyrolysis process. Careful observation indicated that some nanoparticles were anchored on the surface of MWCNTs, and the particle sizes in catalyst a, b and c were approximately estimated to be 15nm, 10 nm and 20nm, respectively. Also, it can be seen that some aggregates (as shown by yellow-circled part ) were formed in catalyst b, and the particle distribution of catalyst a was better than that of catalyst b. While, for catalyst c, large aggregates were found as red-circled part in image c. Generally, the particle size, particle size distribution, particle morphology and etc., were all the factors which could remarkably affect the electrocatalytic activity of a catalyst. Probably, the relatively smaller particle size and the more uniform particle distribution of catalyst a were beneficial to its electrocatalytic activity when compared to other catalysts.

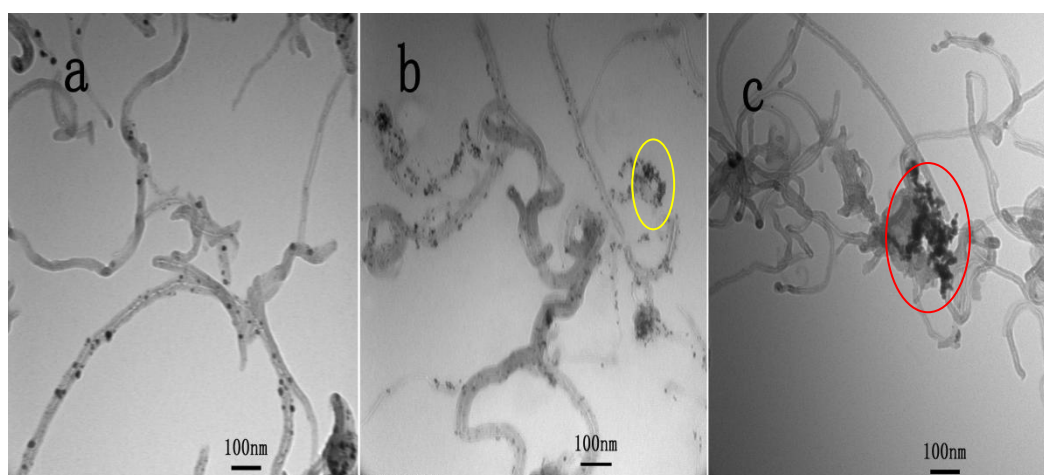


Figure 2. TEM images of the produced catalysts. Image a, b and c corresponded to catalyst a, b and c.

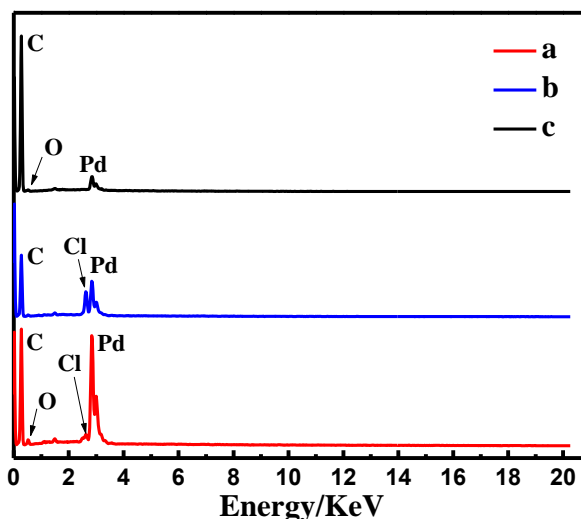
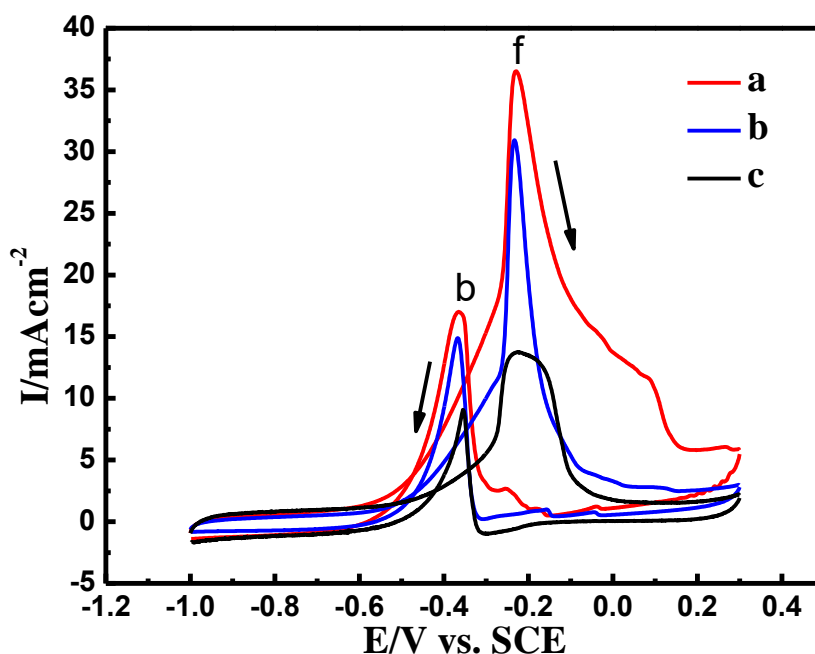


Figure 3. EDS curves of the produced catalysts. Curve a, b and c corresponded to catalyst a, b and c.

To better examine the chemical components of the as-prepared catalysts, EDS analysis was conducted and the results are shown in Fig.3. For catalyst c, compared to the peak of C, the peak belonging to Pd element was too small. It suggested that the content of Pd element in catalyst c was very low, being consistent with XRD analysis (Fig.1). For catalyst a and b, the peaks assigned to the elements of C, Cl and Pd were all exhibited, which also supported the conjecture that some remnants of PdCl<sub>2</sub> were retained in the resultant catalysts. The atomic contents of Pd in catalyst a, b and c were measured to be 26.1%, 5.9% and 2.6%, respectively. That is to say, more amount of Pd element was contained in catalyst a, which could lead to a satisfactory electrocatalytic performance. Theoretically, the atomic content of Pd element in catalyst a should be close to 8.5% if the reaction rate concerning the formation of Pd element in catalyst b was identical to that in catalyst c. Or in other words, the chemical reaction rate occurring in the formation of catalyst a was rather different from those of catalyst b and c. It seemed that the introduction of PdCl<sub>2</sub> as an accelerator had greatly promoted the reaction rate of a chemical reaction between PdO and MWCNTs.

### 3.3 Electrocatalytic performance



**Figure 4.** Cyclic voltammograms measured on the catalysts coated GC electrodes in 1M KOH containing 1M CH<sub>3</sub>OH solution at 50 mV s<sup>-1</sup>. The red, blue and black curves were noted on the catalyst **a**, **b** and **c** coated GC electrode.

The cyclic voltammetry (CV) curves of MOR on the prepared catalysts were recorded at a scanning rate of 50 mV s<sup>-1</sup> in a solution of 1 M KOH containing 1M CH<sub>3</sub>OH and the results are displayed in Fig. 4. Apparently, for all CV curves, two evident oxidation peaks were displayed clearly, namely, one oxidation peak positioned at about ~-0.23V in the positive direction potential sweep (peak f) and one oxidation peak centered at about ~-0.36 V in the negative direction potential sweep (peak b).

b). The shape of CV curves in Fig.4 was very consistent with that of the previously reported CVs of MOR on Pd electrode [3], which also confirmed that all the prepared catalysts had electrocatalytic activities for MOR. Although no much shifting of the peak potential was found in Fig.4, the peak current and onset potential value were rather different from each other. For the oxidation peaks appearing in the positive direction potential sweep (peak f), the peak currents and onset potentials for catalyst a, b and c were estimated to be  $36.7 \text{ mA cm}^{-2}$  and  $-0.53\text{V}$ ,  $31.0 \text{ mA cm}^{-2}$  and  $-0.48\text{V}$ ,  $13.7 \text{ mA cm}^{-2}$  and  $-0.40\text{V}$ , respectively. Therefore, catalyst a exhibited the largest oxidation peak current and the most negative onset potential among all the catalysts, which strongly implied that catalyst a had the best electrocatalytic activity towards MOR. Also, it was reported that the peak f was generally due to the direct electro-oxidation of methanol or the chemisorbed species coming from methanol solution, and the peak b was primarily originated from the electrooxidation of carbonaceous species that were produced in the forward scan [8]. Additionally, it was claimed that the current ratio of peak f to peak b could be employed as an indicator which might reflect the degree of the poisoning tolerance of a catalyst [9,10], and a larger  $I_f/I_b$  ratio commonly corresponded to a larger poisoning tolerance and a better oxidation ability of a catalyst. The current ratios of peak f to peak b were estimated to be 2.1, 1.9 and 1.6, respectively, for catalyst a, b and c. Thus, catalyst a exhibited the best poisoning tolerance among the prepared catalysts. Therefore, it can be inferred that the introduction of  $\text{PdCl}_2$  can greatly enhance the electrocatalytic performance of the pyrolysis products from the system having PdO and MWCNTs, in terms of onset potential and peak current as well as the poisoning tolerance.

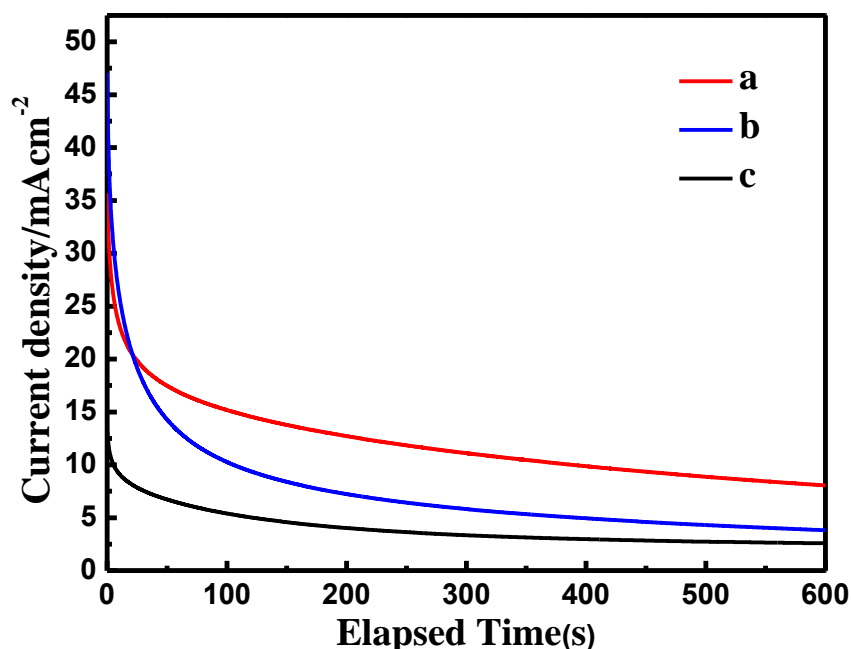


**Figure 5.** Chronoamperometry curves of different catalysts coated GC electrodes measured in 1M KOH +1M  $\text{CH}_3\text{OH}$  at  $-0.24 \text{ V}$ . The red, blue and black curves were recorded on the catalyst a, b and c coated GC electrodes.

The durability is a key factor which can directly decide the service life of an electrocatalyst in a practical fuel cell. Chronoamperometry (CA) is a technique which can be utilized to assess the

durability of an electrocatalyst easily [11]. The CA curves, measured at  $-0.24$  V, of the catalyst-coated GC electrodes in  $1$  M KOH +  $1$  M  $\text{CH}_3\text{OH}$  solution, were given in Fig.5. Generally, the sharp drop of the current density in the initial stage was related to the electric double layer of an electrode, which was mainly influenced by the intermediates adsorbed on the surface of an electrode. And the relatively stable currents appearing in the left measuring period were usually attributed to the electrooxidation of methanol (or called as Faradaic current). Obviously, catalyst a had the largest current density in the total testing period among the three catalysts. For instance, the current densities were roughly estimated to be  $8.0$ ,  $3.7$  and  $2.6$   $\text{mA cm}^{-2}$  at  $600$  s, respectively, for catalyst a, b and c. This result further demonstrated that catalyst a showed the largest polarized current density and the best durability as well as stability among all the synthesized catalysts.

### 3.4 Reasons of the electrocatalytic activities

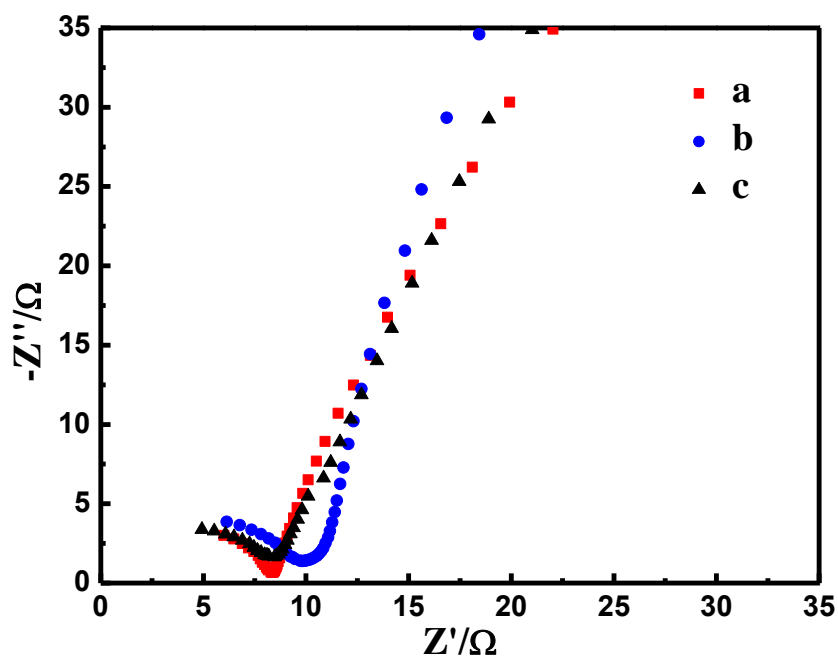


**Figure 6.** Nyquist plots for the catalysts coated GC electrodes which were measured at their open circuit potentials in a solution of  $1$  M KOH +  $1$  M  $\text{CH}_3\text{OH}$ . The red, blue and black curves were recorded on the catalyst **a**, **b** and **c** coated GC electrodes.

Electrochemical impedance spectroscopy (EIS) is a traditional electrochemical technique which has been widely employed to investigate an electrochemical reaction [12], mainly due to its simple operation and better visualization. Nyquist plots, one kind of curves in EIS, for the three electrodes are illustrated in Fig. 6. It should be noted that all above Nyquist plots were measured at their open circuit potentials. Apparently, all curves consisted of a half-open semicircle in the high frequency range and a sloped line in the low frequency region. Commonly, the value of the diameter for the semicircle was directly proportional to the value of charge-transfer resistance ( $R_{ct}$ ) at the electrode/electrolyte interface, and a larger diameter usually matched a bigger value of  $R_{ct}$ . The straight

line in the low frequency region was attributed to the Warburg resistance [12]. The  $R_{ct}$  values for catalyst a, b and c were roughly reckoned to be 8.2  $\Omega$ , 9.3  $\Omega$  and 10.8  $\Omega$ , respectively. Thus, catalyst a owned the smallest value of  $R_{ct}$  among all the catalysts. It strongly demonstrated that catalyst a had a faster electron transfer kinetics than other catalysts, which might lead to a better electrocatalytic performance as compared to catalyst b and c.

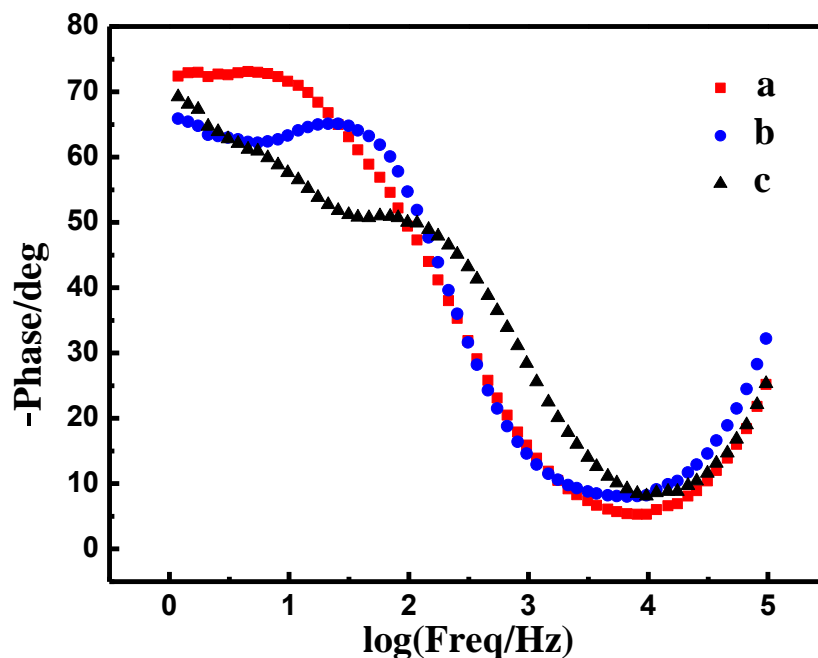


**Figure 7.** Bode plots obtained for the catalysts coated GC electrode which were measured at their open circuit potentials in a solution of 1 M KOH + 1 M CH<sub>3</sub>OH. The red, blue and black curves were recorded on the catalyst **a**, **b** and **c** coated GC electrodes.

To obtain more information of the prepared catalysts, Bode plots are recorded and presented in Fig.7. Clearly, for all electrodes, only one symmetric peak, which generally corresponded to a relaxation process of the electrode/solution interface, was observed in the whole frequency region [13]. The top frequencies for the symmetric peaks of electrode a, b and c were about 2.5Hz, 26Hz and 63Hz, respectively. The existence of relaxation process in the low frequency region was favorable to the charge transfer process, as compared to those relaxation processes occurring in the higher frequency region. Meanwhile, the higher phase angles of the catalyst a coated GC electrode ( $-71^\circ$  at 1Hz) compared to other catalysts ( $-65^\circ$  at 1 Hz for catalyst b,  $-68^\circ$  at 1Hz for catalyst c) also demonstrated that catalyst a had exhibited more capacitive behavior than that of other catalysts because that ideal capacitive systems generally have a phase angle of ca.  $-90^\circ$  [14]. This result effectively testified that the microstructure of the surface of the three catalyst coated GC electrodes was different from each other, and more simple and regular microstructure was possessed by catalyst a.

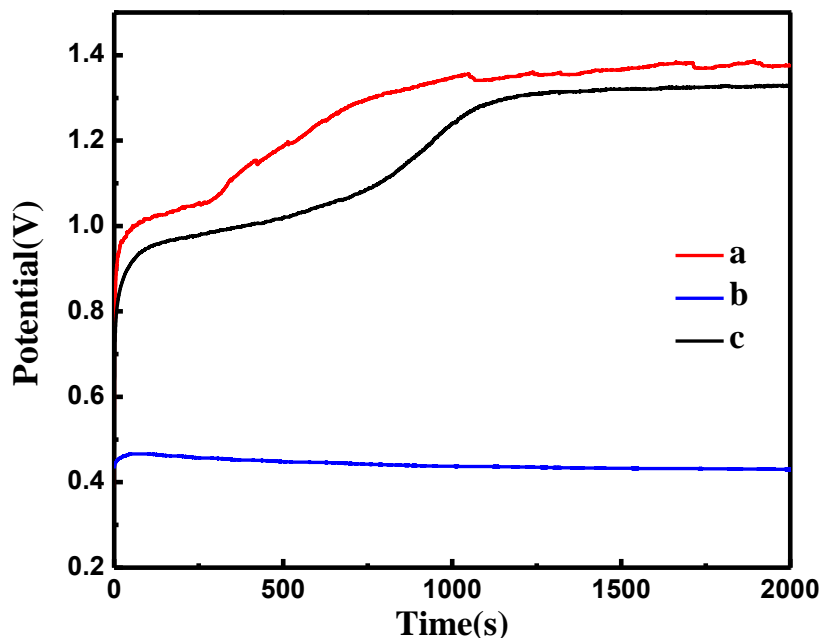


**Figure 8.** Chronopotentiometric curves measured at  $0.02 \text{ A cm}^{-2}$  for the produced catalysts coated GC electrodes in 1 M KOH+1MCH<sub>3</sub>OH. The red, blue and black curves were recorded on the catalyst **a**, **b** and **c** coated GC electrodes.

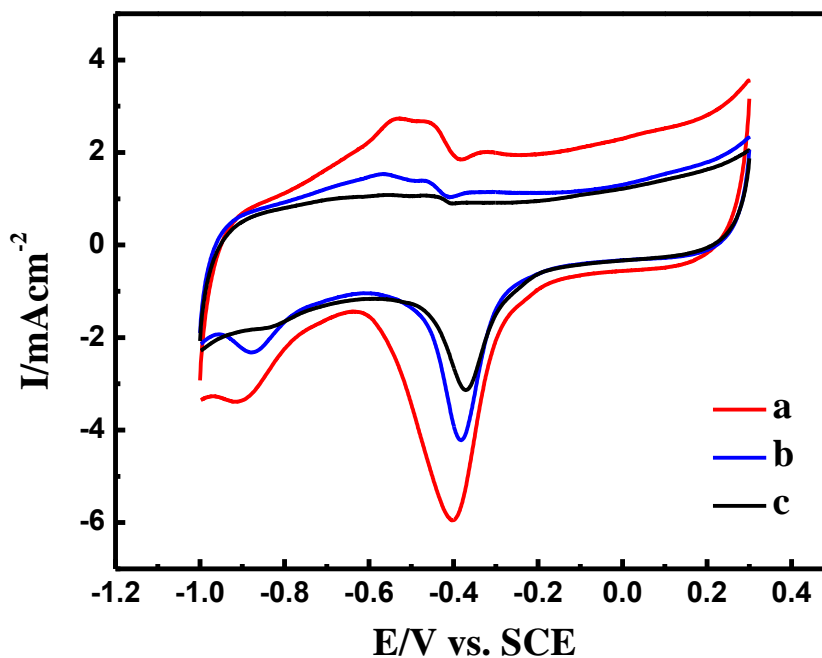


**Figure 9.** Cyclic voltammetry curves recorded on the catalysts coated GC electrodes in 1M KOH solution at the scan rate of  $50 \text{ mV s}^{-1}$ . The red, blue and black curves were obtained on the catalyst **a**, **b** and **c** coated GC electrodes.

Chronopotentiometric (CP) experiments were also carried out with an intention to further analyze the reasons for the enhanced electrocatalytic performance of the prepared catalysts towards

MOR. Fig. 8 shows the chronopotentiometric curves of methanol oxidation on the three kinds of electrodes. In all cases, the electrode potential increased evidently with the testing period when being charged by a positive current, which accorded well with the Tafel equation [15]. Careful observation indicated that electrode a showed the highest electrode potential among all electrodes in the whole testing duration. For example, the electrode potential for electrode a, b and c reached 1.38V, 0.43V and 1.31V at 2000s, respectively. That is to say, electrode a was easier to be polarized to a high potential value as compared to other electrodes. According to the Nernst equation [16], the electrode with a higher electrode potential, generally, corresponded to stronger oxidation ability. Consequently, the methanol oxidation reaction (MOR) may proceed more easily on electrode a than on other electrodes.

To further discuss the possible reasons for the significantly increased electrocatalytic performance, CV curves of the three catalysts coated GC electrodes in 1M KOH were presented in Fig. 9. It should be emphasized that the shape of CV curves in Fig.9 was very similar to that of CV curves on the pure Pd electrode [17]. Hence, the reduction peak emerged at about -0.4V should be due to the electro-reduction of the Pd oxide ( $\text{PdO} + \text{H}_2\text{O} + 2\text{e}^- \leftrightarrow \text{Pd} + 2\text{OH}^-$ ) during the cathodic potential sweep [17]. And the small reduction peak centered at about -0.90V should be originated from the formation of adsorbed hydrogen atoms on the Pd surface, namely,  $\text{Pd} + \text{H}_2\text{O} + \text{e}^- \rightarrow \text{Pd-H}_{\text{ads}} + \text{OH}^-$ , correspondingly, the oxidation peak positioned at about -0.54V should be from the oxidation of adsorbed hydrogen atoms, i.e.,  $\text{Pd-H}_{\text{ads}} + \text{OH}^- \rightarrow \text{Pd} + \text{H}_2\text{O} + \text{e}^-$ . Also, it should be noticed that the oxidation reaction of methanol started at about -0.53V (Fig.4), which just coincided with the small oxidation peak at -0.54V in Fig.9. That is to say, prior to the electrooxidation of methanol, more amounts of fresh Pd atoms were electrochemically produced on the surface of catalyst a, which would accelerate the process of MOR. The presence of the small oxidation peak (at -0.54V) and the large reduction peak (at -0.40V) in Fig.9 also strongly confirmed that much more fresh Pd atoms were prepared on the surface of catalyst a, which might account for its significantly enhanced electrocatalytic performance.

As we know, the mechanism of ethanol oxidation reaction (EOR) on Pd electrode has been well studied in the previous works [17]. And it has been proposed that the adsorption of ethanol molecules on the surface of Pd electrode was the first step in EOR, namely,  $\text{Pd} + \text{CH}_3\text{CH}_2\text{OH} \leftrightarrow \text{Pd}-(\text{CH}_3\text{CH}_2\text{OH})_{\text{ads}}$ . And the second step was an electrochemical reaction, i.e.,  $\text{Pd}-(\text{CH}_3\text{CH}_2\text{OH})_{\text{ads}} + 3\text{OH}^- \rightarrow \text{Pd}-(\text{CH}_3\text{CO})_{\text{ads}} + 3\text{H}_2\text{O} + 3\text{e}^-$  [17]. Probably, in a similar way, the adsorption of methanol molecules on the Pd surface is the first step of MOR. Evidently, the fresh Pd atoms that were released at -0.54V were favorable to the adsorption of methanol molecules as compared to the stale Pd surface. Also, as addressed above, the presence of the large reduction peak at -0.9V also indicated that more  $\text{OH}^-$  groups were created in the vicinity of the surface of catalyst a, which was advantageous to the second step of MOR, i.e., an electrochemical reaction, basing on the theory of equilibrium drift. As a result, catalyst a exhibited the best electrocatalytic performance among all the synthesized catalysts.

#### 4. CONCLUSION

For the first time, the electrocatalytic performance of the pyrolysis products of the mixture having PdO+PCl<sub>2</sub>+MWCNTs was investigated. And in this work, three kinds of catalysts were

prepared by using a very simple method of pyrolysis. The prepared catalysts were thoroughly characterized by using XRD and TEM. XRD patterns substantially indicated that after the pyrolysis process new substances of metallic Pd were produced. TEM images proved that some nanoparticles with a size less than 20nm were immobilized on the surface of MWCNTs after the pyrolysis process. The results of the electrochemical experiments verified that catalyst a, i.e., the pyrolysis products of the mixture having PdO+PdCl<sub>2</sub>+MWCNTs, showed the best electrocatalytic activity for MOR among all the synthesized catalysts. Showing the fact, that the electrocatalytic activity of catalyst a (the pyrolysis product of the mixture containing PdO+PdCl<sub>2</sub>+MWCNTs) was much better than other catalysts, was the major contribution of this work, which implied that PdCl<sub>2</sub> could probably be employed as an additive agent to promote the electrocatalytic ability of a Pd-based catalyst.

#### ACKNOWLEDGEMENTS

This work was financially supported by the State Key Program of National Natural Science of China (21236003), National Natural Science Foundation of China (No. 21173066, 21476022, & 21676022), Natural Science Foundation of Hebei Province of China (No.B2011205014 and B2015205150), the Fundamental Research Funds for the Central Universities (JD1515, JD1612 and YS1406), Beijing Higher Education Young Elite Teacher Project (YETP0509), BUCT Fund for Disciplines Construction and Development (No. XK1531).

#### References

1. B. Y. Xia, H. B. Wu, X. Wang and X. W. Lou, *J. Am. Chem. Soc.*, 134 (2012) 13934.
2. A. A. Ensafi, M. Jafari-Asl, B. Rezaei, M. M. Abarghoui and H. Farrokhpour, *J. Power Sources*, 282 (2015) 452.
3. J. Wang, N. Cheng, M. Norouzi Banis, B. Xiao, A. Riese and X. Sun, *Electrochim. Acta*, 185 (2015) 267.
4. H. Erikson, M. Lüsi, A. Sarapuu, K. Tammeveski, J. Solla-Gullón and J. M. Feliu, *Electrochim. Acta*, 188 (2016) 301.
5. H. Rostami, A. A. Rostami and A. Omrani, *Electrochim. Acta*, 194 (2016) 431.
6. K. Ding, Y. Wang, H. Yang, C. Zheng, Y. Cao, H. Wei, Y. Wang and Z. Guo, *Electrochim. Acta*, 100 (2013) 147.
7. K. Ding, Y. Zhao, Y. Li, J. Zhao, Y. Chen, Y. Wang and Z. Guo, *Int. J. Electrochem. Sci.*, 10 (2015) 969.
8. Y.-H. Qin, Y. Zhuang, R.-L. Lv, T.-L. Wang, W.-G. Wang and C.-W. Wang, *Electrochim. Acta*, 154 (2015) 77.
9. T.C. Deivaraj, W. Chen and J.Y. Lee, *J. Mater. Chem.*, 13(2003) 2555.
10. K. Ding, Y. Zhao, L. Liu, Y. Cao, Q. Wang, H. Gu, X. Yan and Z. Guo, *Int. J. Hydrogen Energ.*, 39 (2014) 17622.
11. K. Ding, Y. Li, Y. Zhao, J. Zhao, Y. Chen, Q. Wang, *Int. J. Electrochem. Sci.*, 10 (2015) 8844.
12. K. Ding, Z. Jia, Q. Wang, X. He, N. Tian, R. Tong and X. Wang, *J. Electroanal. Chem.*, 513 (2001) 67.
13. C. Hu, S. Yuan and S. Hu, *Electrochim. Acta*, 51(2006) 3013.
14. K. Ding, L. Liu, Y. Cao, X. Yan, H. Wei and Z. Guo, *Int. J. Hydrogen Energ.*, 39 (2014) 7326.
15. K. Kodama, R. Jinnouchi, T. Suzuki, T. Hatanaka and Y. Morimoto, *Electrochim. Acta*, 78 (2012) 592.

16. S. Carrara, C. Baj-Rossi, C. Boero and G. D. Micheli, *Electrochim. Acta*, 128 (2014) 102.
17. Z.X. Liang, T.S. Zhao, J.B. Xu and L.D. Zhu, *Electrochim. Acta*, 54 (2009) 2203.

© 2017 The Authors. Published by ESG ([www.electrochemsci.org](http://www.electrochemsci.org)). This article is an open access article distributed under the terms and conditions of the Creative Commons Attribution license (<http://creativecommons.org/licenses/by/4.0/>).